Modeling of Unsteady-State Cake Formation on a Fracture in Produced Water Re-Injection Process (PWRI)

Adli, Atieh*+; Rashidi, Fariborz; Farajzadeh, Rouhollah
Chemical Engineering Faculty, Amirkabir University of Technology, Tehran, I.R. IRAN

ABSTRACT: *In petroleum production, Produced Water Re-Injection (PWRI) has earned much interest among disposal methods of the produced water. However, presence of the contaminants in the produced waters usually results in formation damage in well bores and their surrounding fracture systems. In the present study, modeling of external cake formation on a fracture in unsteady-state conditions is discussed. The existing force vectors of different nature are analyzed in detail at first, as the second step force and fluid mass balances specific to the case are derived. Finally, by solving the formulated governing equations, cake thickness, permeate velocity and cross flow velocity profiles in unsteady-state conditions are obtained.*

KEY WORDS: *External cake, Produced water, Porous media, Filtration.*

INTRODUCTION

Due to importance of the environmental issues and the huge amount of produced subsurface waters, the subsurface re-injection of produced water has already earned a lot of attention. The process is usually accompanied by formation damage. This damage decomposes to internal filtration into the formation and also an external filter cake buildup.

The study of external filter cake in the field of petroleum engineering dates back to the 1940s [1] and was continued with the works of *Khatib* [2], *Civan* [3] and *Sharma et. al.* [4]. More fundamental research into the buildup of external filter cake can be found in the fields of colloid science [5] and membrane technology [6], where phenomenological models are replaced with fundamental models incorporating force analysis.

The principal of filter cake buildup is based on the multilayer deposition of the suspended particles carried by the permeate flux. Yet, experimental observations indicate that not all of the particles transported by the permeate flux to the interface are deposited [7]. Different authors attempted to explain the back transport of particles using different physical models [8] among which are: concentration polarization of reverse osmosis based on *Stokes-Einstein* diffusion; also based on shear induced diffusion; and inertial lift. *Song & Elimelech* [9] introduced a general model that can account for both the concentration polarization layer and external cake formation by considering both the hydrodynamic and thermal energies of the system and identifying an appropriate critical filtration number.

The aforementioned works [3], [5], [6] calculate the cake thickness from a force balance in the light of assuming a constant average permeate flow along the well bore/channel. Thus, the predictions obtained can

* *To whom correspondence should be addressed.*
+ *E-mail: atieh.adli@gmail.com*
1021-9986/10/2/143 8/$/2.80

only be applied to short geometries where a constant permeate velocity is applicable. Long well bores along thick geological beds or deep penetrated fracture openings can not be modeled without accounting for the varying leak off effect.

Modeling of external filter cake in a fracture for steady-state conditions along with experimental data are given in reference [10]. As a further study, this paper investigates modeling of external filter cake on a fracture face in unsteady-state conditions. The asymptotic solutions are compared with the steady solution presented in *Farajzadeh* [10].

MODELING OF UNSTEADY STATE EXTERNAL FILTER CAKE IN A FRACTURE

In this paper modeling conditions are taken the same as Ref. [10] and [11] in which the injected fluid is a suspension of hematite particles in water and porous medium is Bentheim sandstone. See table 1 for the details of modeling conditions.

Table 1: Modeling Conditions.

Cake Permeability (k_c)	10 μD
Porous Medium Permeability (k)	1.5 D
Porous Medium Thickness (l)	10 cm
Back Pressure (pressure at the end of the channel)	5.0 bar
Cake Porosity (φ_c)	0.4
Gamma (γ=f/w)	8.33 E-3
Channel Length (L)	1.0 m
Channel Height (H)	5.0 mm
Channel Width (W)	20.0 mm
Injection Rate (Q_0)	2.78 E-6 m^3/sec
Inlet Concentration (c_0)	40 ppm
Particle Radius (a)	*2.0 μm*
PH of Injected Fluid	5.5±0.1

Assumptions

Fig. 1 shows the experimental setup. In this Figure, h is thickness of the cake, L is the length of setup in axial direction, u_p is the permeate velocity and $\bar{u}_{cf}$ is the cross flow velocity. For this modeling like Refs. [10] and [11] the following assumptions are considered:

- Changes of velocity in y direction are neglected
- Shear forces are just in x direction
- The velocity profile in any section of the setup is fully developed
- Porosity of cake is constant
- Filter cake has a constant permeability k_c
- Porous medium has a constant permeability k
- The injected suspension is dilute and Newton's law is applicable
- The temperature is constant
- All particles have the same diameter

In addition, for the unsteady-state case another condition was added to the above set. That is, initial filtrations prior to the solution are neglected and that zero time of modeling is the time that external cake starts to build up.

Forces acting on a particle at the surface of the filter cake

The forces acting on a particle deposited at the surface of the cake, depicted in Fig. 2, are cross flow and permeate viscous drags, lift, gravity, diffusion, interparticle (electrostatic and van der Waals) and friction forces. *Al-Abduwani et al.* [11] performed a sensitivity analysis under the injection conditions of the experiments and obtained the order of magnitude of different present forces as follows: F_{cf} (Cross Flow Drag) ~10^{-3}N, F_p (Permeate Drag) ~10^{-11}N, F_g (Gravity) ~10^{-14}N and F_l (Lift) ~10^{-19}N.

In this paper, the order of magnitude for electrostatic and van der Waals forces are obtained as follow: F_e (Electrostatic) ~10^{-12}N and F_{vdm} (van der Waals) ~10^{-14}N. See Appendix A for details.

It is evident from the comparison of different forces that cross flow drag, permeate drag and electrostatic forces are the dominant ones. Friction forces are also important because they are proportional to the normal forces. Though there has been an evaluation of Electrostatic force effectiveness, but due to the complexity added to the physics of the problem like in Ref. [11], in this paper also this force was neglected.

Force balance

Force balance is written for a particle at the surface of cake. Before writing force balances, effective forces should be formulated. In Ref. [11] general form of cross flow and permeate drag forces are given as:

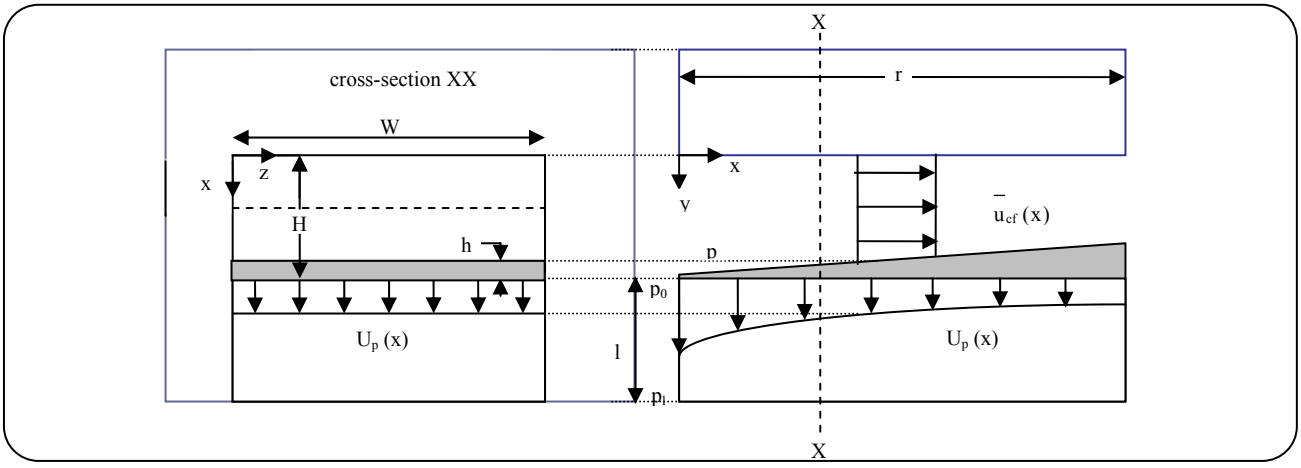

Fig. 1: Schematic of cake formation on a fracture.

Cross flow drag force:

$$F_{cf} = w\pi a^2 \frac{\mu \bar{u}_{cf}}{(H-h)} \quad (1)$$

Permeate drag force:

$$F_p = 6\pi\mu a u_p \quad (2)$$

Where w is a proportionality factor, μ is the viscosity of fluid, a is the particle radius, $\bar{u}_{cf}$ is the average cross flow velocity at a given cross-section, H is the height of the channel, h is the thickness of the cake at a given cross-section and u_p is the permeate velocity at a given cross-section.

Friction force is proportional to the summation of normal forces. Therefore, friction force is given as:

$$F_f = f.F_N \quad (3)$$

In which f is the frictional coefficient.

Force balance for a particle at the surface of cake is written as follow:

$$F_{cf} = f \times F_p \quad (4)$$

Substitution of Eqs. (1) and (2) into Eq. (4) yields Eq. (5):

$$\frac{\bar{u}_{cf}}{u_p} = \frac{6f}{wa}(H-h) \quad (5)$$

Fluid mass balanc

The other equation that is needed for modeling is the fluid mass balance. Fig. 3 is used for writing mass balance.

Mass balance for fluid can be written as:

$$(u_{cf}(H-h)W\rho)_{in} = (u_{cf}(H-h)W\rho)_{out} + \frac{u_{p,1}+u_{p,2}}{2}\rho\Delta xW + \frac{\partial}{\partial t}(\rho(H-h)\Delta xW + \varphi_c\rho h\Delta xW) \quad (6)$$

When $\Delta x \to 0$ Eq. (6) change to:

$$-\frac{\partial(u_{cf}(H-h))}{\partial x} = u_p + (1-\varphi_c)\frac{\partial(H-h)}{\partial t} \quad (7)$$

Cake thickness equation

Permeate velocity and pressure equations are needed for obtaining the cake thickness equation.

Al-Abduwani et al. [11] obtained permeate velocity as follow:

$$u_p = \left(\frac{h}{k_c} + \frac{l}{k}\right)\frac{p-p_l}{\mu} \quad (8)$$

Where k and k_c are the permeability of the porous medium and the filter cake respectively. The parameter l is the thickness of porous medium. p and p_l are the pressure in the channel and the pressure of the porous medium at effluent side respectively (Fig.1). *Farajzadeh* [10] obtained pressure equation as follow:

$$\frac{dp}{dx} = -\frac{12\mu\bar{u}_{cf}}{(H-h)^2} \quad (9)$$

Therefore cake thickness equation is obtained as follow: (for more details see Appendix B)

$$\frac{\partial h}{\partial t} = \frac{u_p}{(1-\varphi_c)} - \frac{u_{cf}}{(1-\varphi_c)}\left[\frac{72\gamma k_c}{a(h+\Theta)} + \left(2+\frac{H-h}{h+\Theta}\right)\frac{dh}{dx}\right] \quad (10)$$

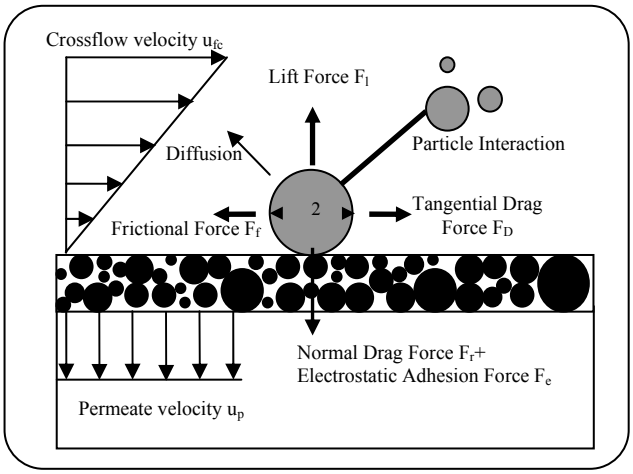

Fig. 2: Forces acting on a particle deposited on the surface of the cake [10].

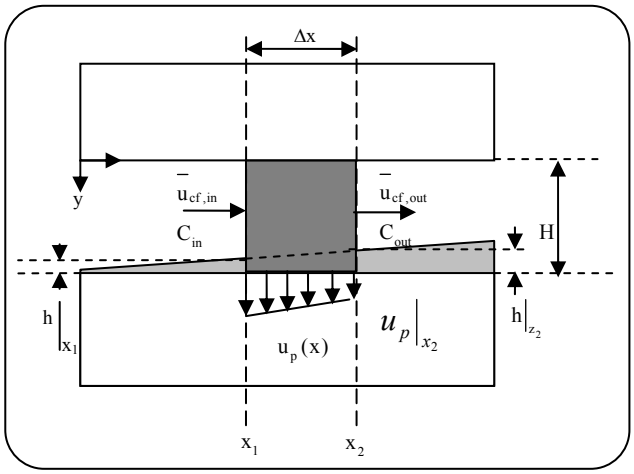

Fig. 3: Element used for mass balance.

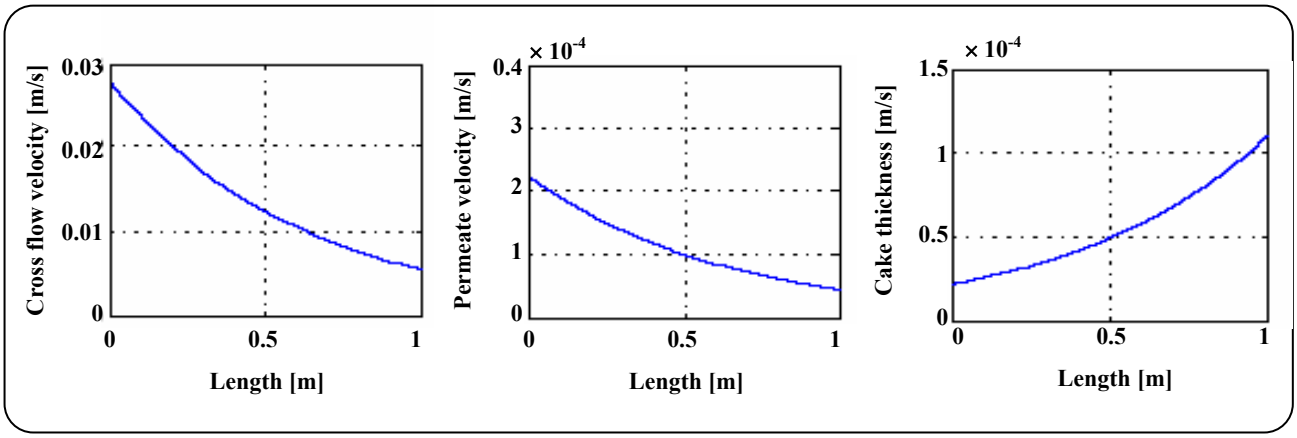

Fig. 4: Profiles in steady condition [10], [11].

The parameters Θ and γ are introduced in Appendix B.

Cake thickness increase with time until cross flow drag force is less than friction force. When cross flow drag force becomes more than friction force, cake thickness converges to the steady condition and does not increase more with time. So in addition to Eq. (10) this condition must be considered similar to when the cake thickness is smaller than cake thickness in steady condition.

Finding cake thickness in steady condition is as follow (in steady condition cross flow drag force is more than friction force):

$$F_{cf} > F_f \tag{11}$$

Substitution of cross flow drag and friction forces into Eq. (11) yields Eq. (12):

$$\frac{\bar{u}_{cf}}{u_p} > \frac{6f}{wa}(H-h) \tag{12}$$

With substituting equation (B-1) and (B-6) into Eq. (12) and knowing flow rate (Q) at the beginning of the channel we can find maximum of cake thickness (h_o). So until cake thickness is less than h_o we find cake thickness from Eq. (10) and when cake thickness is equal or more than h_o we put cake thickness equal to h_o. So that there is no problem in stability condition.

RESULTS OF MODELING

Cake thickness, permeate velocity and cross flow velocity profiles in steady condition were obtained from Refs. [10] and [11] as are illustrated in Fig.4.

Farajzadeh [10] showed that in steady conditions pressure change along the channel is not significant and

it could be assumed constant. For the unsteady-state conditions also pressure is assumed to be constant. Although this is not a true assumption, it could be considered because cake thickness is so small vs. channel height. For getting cake thickness, permeate velocity and cross flow velocity profiles in unsteady conditions, and equations (10), (8) and (5) need to be solved. As analytical solution for these equations is not possible, a numerical approach was persuaded through computer programmings using the MATLAB algebraic system. The results are shown in Figs. 5, 6 and 7. These figure show that after a definite period of time cake thickness, permeate velocity and cross flow velocity profiles converge to steady profiles of Fig. 4. This way the results of modeling in unsteady condition and the results of modeling in steady condition confirm each other. The steady-state solutions in turn are compared against the experimental studies in RefS. [10] and [11].

Fig.5 shows that cake thickness increases with time because when the time increases, the number of particles that settle on the surface of cake increase. Also for a specific time cake thickness increases along the channel, this is a direct consequence of shear forces caused by cross flow velocity. Also you can see that the speed of convergence to steady state condition decreases along the channel. This is because of decreasing flow velocity along the channel that causes decrease in shear forces.

Fig. 6 shows that permeate velocity decreases with time and for a specific time it decreases along the channel, these are because of increasing cake thickness that leads to increasing resistance against flow permeation into the porous medium. And finally, Fig. 7 also shows that cross flow velocity decreases with time and for a specific time it decreases along the channel, these are because of leak off of the liquid along the channel. For permeate velocity and cross flow velocity like cake thickness, the speed of convergence to steady state condition decrease along the channel. This is a direct consequence of cake thickness, because cake thickness has effect the permeate velocity and cross flow velocity and cause that these two parameters having same behavior.

The growth of the cake reduces the cross section available for the cross flow to pass along the channel, thus the shear rate increases, causing a steady state cake to eventually be reached when the rate of particle convection to the cake surface is balanced by shear back transport of the particles.

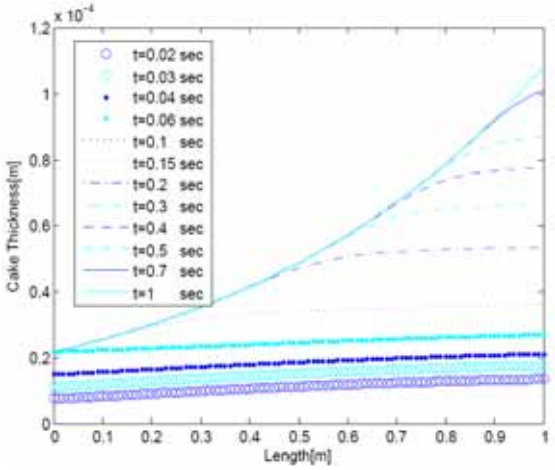

Fig. 5: Cake thickness profile in unsteady condition.

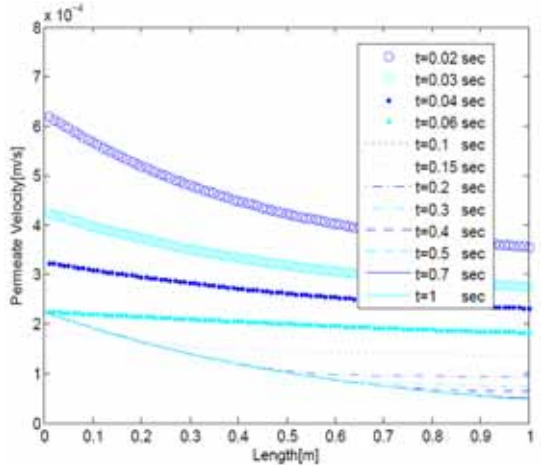

Fig. 6: Permeate velocity profile in unsteady condition.

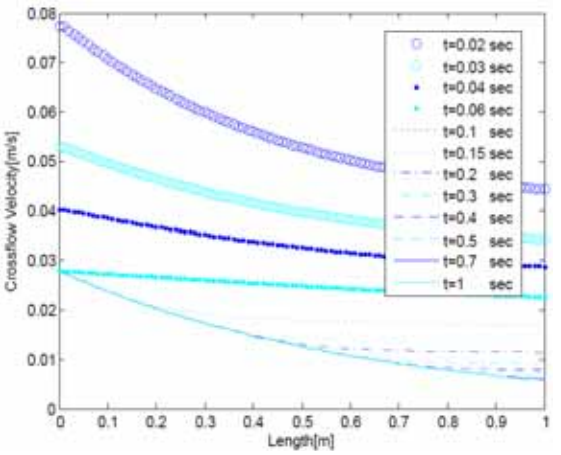

Fig. 7: Cross flow velocity profile in unsteady condition.

CONCLUSIONS

Produced Water Re-Injection (PWRI) process generally leads to damage of the formations. The problems of formation damage due to PWRI can be decomposed into separate distinct problems. These include internal filtration and external filter cake buildup. Force analysis shows that, in addition to the drag and friction forces that act on a particle in injected fluid, electrostatic force is also an effective force. But if electrostatic force comes to modeling, it will cause a lot of complications. Therefore, electrostatic forces are neglected like pervious studies in the literature. In this paper modeling of external cake in unsteady condition confirms the results of modeling in steady condition and unsteady profile after a period of time converges to steady solution profiles.

Appendix A: Derivation of the equations for electrostatic and van der Waals forces

The interaction between colloidal particles is usually given in term of potential. The formulation of the electrostatic force used in this article is that adopted by *Joachim & Schulze* [12] and originally proposed by *Hogg*.

$$U_e = \pi\varepsilon_0\varepsilon_r a(\psi_1{}^2 + \psi_2{}^2)\times \left\{\frac{2\psi_1\psi_2}{(\psi_1{}^2+\psi_2{}^2)}\mathrm{Ln}\left(\frac{1+e^{-\kappa R}}{1-e^{-\kappa R}}\right)+\mathrm{Ln}(1-e^{-2\kappa R})\right\} \quad (A\text{-}1)$$

At later deposition time when a significant number of multi-layers have been deposited, the surface charge of the collector grain becomes masked. Thus the depositing particles effectively interact with identically charged deposited particles and (A-1) reduces as follows:

$$U_e = 2\psi^2\pi\varepsilon_0\varepsilon_r a\left\{\mathrm{Ln}\left(\frac{1+e^{-\kappa R}}{1-e^{-\kappa R}}\right)+\mathrm{Ln}(1-e^{-2\kappa R})\right\}$$

Or:

$$U_e = 2\psi^2\pi\varepsilon_0\varepsilon_r a\mathrm{Ln}\left\{\frac{(1+e^{-\kappa R})(1-e^{-\kappa R})(1+e^{-\kappa R})}{(1-e^{-\kappa R})}\right\}$$

$$\Rightarrow \quad U_e = 4\psi^2\pi\varepsilon_0\varepsilon_r a\mathrm{Ln}\left[1+e^{-\kappa R}\right] \quad (A\text{-}2)$$

Since $F_e = -\frac{\partial U_e}{\partial R}$ then electrostatic force can be calculated with the following equation:

$$F_e = 4\psi^2\pi\varepsilon_0\varepsilon_r a\kappa\frac{e^{-\kappa R}}{1+e^{-\kappa R}} \quad (A\text{-}3)$$

The formulation of the van der Waals force used in this article was given by *Hamaker* [13]:

$$U_{vdw} = -\frac{A}{6}\left[\frac{2a_1a_2}{R^2-4a_1a_2}+\frac{2a_1a_2}{R^2}+\mathrm{Ln}\left(\frac{R^2-4a_1a_2}{R^2}\right)\right] \quad (A\text{-}4)$$

For two particles of the same size and when the distance between particles surface is much less than the radius of the particle, equation (A-4) becomes:

$$U_{vdw} = -\frac{Aa}{12}\frac{1}{R-2a} \quad (A\text{-}5)$$

Since $F_{vdw} = -\frac{\partial U_{vdw}}{\partial R}$ then van der Waals force can be calculated with the following equation:

$$F_{vdw} = \frac{-Aa}{12}\frac{1}{(R-2a)^2} \quad (A\text{-}6)$$

In (A-3) and (A-6) equations, a is the radius of the particle, A is Hamaker constant, the amount of A for this system is 3.4×10^{-20} J [12], $\varepsilon_0 = 8.85\times10^{-12}\,C^2J^{-1}m^{-1}$ is the absolute permittivity of the free space, ε_r is the dielectric constant of the fluid between particles (for water is 78.5), ψ is stern potential and the measurable value of zeta potential ξ can be used instead of that and for this system zeta potential is 20mV [14], κ is the reciprocal of the thickness double layer and can be estimated by :

$$\kappa = \left[\frac{e^2\sum n_i{}^0 z_i{}^0}{\varepsilon_0\varepsilon_r k_B T}\right]^{\frac{1}{2}} \quad (A\text{-}7)$$

Where e is the unit electrical charge (1.6×10^{-19}C), n_i^0 and z_i are the number of ions per unit volume in the bulk solution and valence of type I, respectively. k_B is the Boltzman constant ($1.4\times10^{-23}JK^{-1}$) and T is the absolute temperature in Kelvin.

Tent & Nijenhuis [15] obtained the shortest distance R between two neighboring particles by proposing a hexagonal packing structure of the deposited particles:

$$R = \left\{\left[\frac{\pi}{K_1(1-\varepsilon_0)}\right]^{0.33}-1\right\}d_p \quad (A\text{-}8)$$

McDonogh et al indicated that the only interparticle forces between neighboring particles of filter cake should be considered. They proposed the following equation to evaluate K_l with assuming the hexagonal packing structure of the deposited particles:

$$K_l = 3\cos\theta \tag{A-9}$$

Where θ varies from 0 to 90 and for hexagonal packing θ is 54.7°.

Appendix B: Derivation of the cake thickness equation

Volumetric flow rate in channel, Q, is given by:

$$Q = u_{cf}(H-h)W \tag{B-1}$$

Substituting equation (B-1) into equation (7) yields:

$$-\frac{\partial Q}{\partial x} = u_p W + (1-\varphi_c)W\frac{\partial(H-h)}{\partial t} \tag{B-2}$$

Introducing the following parameters:

$$\Psi = \frac{k_c(p-p_l)}{\mu} \tag{B-3}$$

$$\Theta = \frac{k_c}{k}l \tag{B-4}$$

$$\gamma = \frac{f}{w} \tag{B-5}$$

And substituting them in Eqs. (5) and (8) yields:

$$u_p = \frac{\Psi}{h+\Theta} \tag{B-6}$$

$$\frac{\bar{u}_{cf}}{u_p} = \frac{6\gamma}{a}(H-h) \tag{B-7}$$

Substituting (B-6) and (B-1) into (B-7) yields:

$$\frac{\dfrac{Q}{(H-h)W}}{\dfrac{\Psi}{h+\Theta}} = \frac{6\gamma}{a}(H-h)$$

Then volumetric flow rate is stated as follow:

$$Q = \frac{6\gamma W}{a}\frac{\Psi(H-h)^2}{h+\Theta} \tag{B-8}$$

Therefore:

$$\frac{\partial Q}{\partial x} = \frac{6\gamma W}{a}\times \tag{B-9}$$
$$\left[\frac{\left[(H-h)^2\frac{d\Psi}{dx} - 2\Psi(H-h)\frac{dh}{dx}\right](h+\Theta) - \Psi(H-h)^2\frac{dh}{dx}}{(h+\Theta)^2}\right]$$

Equating (B-9) and (B-2) yields:

$$-u_p W - (1-\varphi_c)W\frac{\partial(H-h)}{\partial t} = \tag{B-10}$$
$$\frac{6\gamma W}{a}\left[\frac{(H-h)^2}{(h+\Theta)}\frac{d\Psi}{dx} - \left[\frac{2\Psi(H-h)}{(h+\Theta)} + \frac{\Psi(H-h)^2}{(h+\Theta)^2}\right]\frac{dh}{dx}\right]$$

Substituting (B-7) and (B-6) into (9) yields:

$$\frac{dp}{dx} = -\frac{72\gamma\mu\Psi}{a(H-h)(h+\Theta)} \tag{B-11}$$

Substituting (B-3) into (B-11) yields:

$$\frac{1}{\Psi}\frac{d\Psi}{dx} = -\frac{72\gamma k_c}{a(H-h)(h+\Theta)} \tag{B-12}$$

Substituting (B-12) into (B-10) yields:

$$(1-\varphi_c)\frac{\partial h}{\partial t} = u_p + \tag{B-13}$$
$$\frac{6\gamma}{a}\left[\frac{(H-h)^2}{(h+\Theta)}\left(-\frac{72\gamma k_c\Psi}{a(H-h)(h+\Theta)}\right) - \left[\frac{2\Psi(H-h)}{(h+\Theta)} + \frac{\Psi(H-h)^2}{(h+\Theta)^2}\right]\frac{dh}{dx}\right]$$

After some simplification and substituting (B-7) and (B-6) into (B-13) this equation change as follow:

$$\frac{\partial h}{\partial t} = \frac{u_p}{(1-\varphi_c)} - \tag{B-14}$$
$$\frac{u_{cf}}{(1-\varphi_c)}\left[\frac{72\gamma k_c}{a(h+\Theta)} + \left(2 + \frac{H-h}{h+\Theta}\right)\frac{dh}{dx}\right]$$

Received : Dec. 1, 2008 ; Accepted : Dec. 21, 2009

REFERENCES

[1] Williams.M, 1940, Radial Filtration of Drilling Muds, Trans. *AIME*,136, p. 57.

[2] Khatib Z, Prediction of Formation Damage Due to Suspended Solids: Modeling Approach of Filter Cake Buildup in Injectors, "in SPE 69th Annual

Technical Conference and Exhibition", New Oreleans, LA, U.S.A, SPE 28488 (1994).

[3] Civan F., Phenomenological Filtration Model for Highly Compressible Filter Cakes Involving Non-Dary Flow, "in 1999 SPE Mid-Continent Operations Symposium", Oklahoma City, U.S.A, SPE 52147 (1999).

[4] Pang S., Sharma M.M., "A Model for Predicting Injectivity Decline in Water Injection Wells", *SPEFE*, pp. 194-201 (1997).

[5] Jiao D., Sharma M.M., Mechanism of Cake Buildup in Crossflow Filtration of Colloidal Suspensions, *Journal of Colloid and Interface Science*, **162**, p. 454-462 (1994).

[6] Altmann J., Ripperger S., Particle Deposition and Layer Formation at the Crossflow Microfiltration, *Journal of Membrane Science*, **124**, p. 119 (1997).

[7] Stamatakis K., Tien C., A Simple Model of Cross-Flow Filtration Based on Particle Adhesion, *AIChE J.*, **39**(8), pp.1292-1302 (1993).

[8] Belfort G., Davis R.H., Zydney A.L., The Behavior of Suspensions and Macromolecular Solutions in Crossflow Microfiltration, *Journal of Membrane Science*, **96**, p. 1 (1994) .

[9] Song L., Elimelech M., Theory of Concentration Polarization in Crossflow Filtration, *Journal of the Chemical Society*, *Faraday Transactions*, **91**(19), p. 3389 (1995).

[10] Farajzadeh R., Produced Water Re-Injection (PWRI), an Experimental Investigation into Internal Filtration and External Cake Build-up, {Ms Thesis}, Delft University of Technology (2004).

[11] AlAbduwani F.A.H., Bedrikovetsky P., Farajzadeh R., VandenBroek W.M.G.T., CurrieP K., External Filter Cake Erosion: Mathematical Model and Experimental Study, *SPE94635* (2005).

[12] Joachim.H, Schulze, Physico-Chemical Elementary Process in Flotation; an Analysis from the Point of View of Colloid Science Including Process Engineering Consideration, chap4, Elsevier Pub. Co, pp.84-88 (1984).

[13] Hamaker H.C., The London-van der Waals Attraction between Spherical Particles, *physica*, **4**, p. 1058 (1937).

[14] Zhonghua Pan, Somasundaran P., Turro N.J., Steffen Jockusch, Interaction of Cationic Dendrimers with Hematite Mineral, *Colloids and surfaces* , **238**, p. 123 (2004).

[15] Tent V.A., Nijenhuis, K.T., Turbidity Study of the Process of Film Formation of Polymer Particles in Drying Thin Films of Acrylic Lattice, *J. Colloid and interface science*, **150**, p. 97 (1992).